

Fabrication, characterization, and adsorption capacity of Fe₃O₄/graphene oxide nanocomposites for nickel removal

- Nguyen Huu Hieu
- Hoang Minh Nam
- Phan Thi Hoai Diem

Ho Chi Minh city University of Technology, VNU-HCM

(Manuscript Received on July, 2016, Manuscript Revised on September, 2016)

ABSTRACT

In this research, graphene oxide (GO) was synthesized via modified Hummers' method and for the preparation of Fe₃O₄/GO nanocomposites by impregnation method. Characterization of the nanocomposites was performed by X-ray diffraction, Fourier transform infrared spectroscopy, transmission electron microscope, specific surface area, and vibrating sample magnetometer. The

concentration of Ni (II) ion in solutions was determined using UV-Visible spectrophotometer. The adsorption capacity for Ni (II) removal was examined with respect to pH effect, kinetic data and equilibrium isotherms in batch experiments. The maximum adsorption capacity of the Fe₃O₄/GO estimated with the Langmuir-isotherm model for Ni (II) was 27.62 mg/g at room temperature.

Keywords: Fe₃O₄, graphene oxide, nanocomposite, adsorption, nickel.

1. INTRODUCTION

Graphene (GE) is a two dimensional material that has between one and ten layers of sp²-hybridized carbon atoms arranged in six-membered rings. The length of bonds of GE is 1.42 Å [1]. Single layer GE nanosheet was first obtained by mechanical exfoliation ("Scotch-tape" method) of bulk graphite [2]. Besides, GE sheets have also been fabricated by other methods such as metal ion intercalation, liquid phase exfoliation of graphite, chemical vapor deposition, chemical reduction-oxidation of graphite. Graphene oxide (GO) is a product of

graphite oxidation, is often used to make GE. GO refers to GE with oxygen-containing functional groups as epoxy (C-O-C), hydroxyl (OH), carbonyl (C=O) groups on basal planes and carboxyl (COOH) groups on edges [3]. Therefore, it can be easily exfoliated and functionalized to form homogeneous suspensions in both water and organic solvents. The existence of oxygen functional groups and aromatic sp² domain allows GO to participate in a wide range of bonding interactions. GO has attracted significant attention because of its advantages, such as a large surface area, more activated

functionalized sites, easy preparation, and good biocompatibility. These features ensure that GO can be rapid and efficient removal heavy metal ions such as Ni^{2+} , As^{2+} , Cd^{2+} , etc. However, separating and recycling of GO turn out to be a challenge because of their small size. In addition, the π - π interactions between neighboring sheets might lead to serious agglomeration and restacking, which result in the loss of effective surface area and low adsorption capacity [4]. In order to solve these problems, Fe_3O_4 was added into GO sheets for the efficient removal of heavy metal ions due to the high loading capacity and easy manipulation by external magnets. The magnetic property, 2D structure, and existence of active sites make $\text{Fe}_3\text{O}_4/\text{GO}$ nanocomposites a potential adsorbent for treatment of heavy metal contaminated wastewater.

In this work, $\text{Fe}_3\text{O}_4/\text{GO}$ nanocomposites were synthesized, characterized, and investigated the adsorption capacity for Ni^{2+} ions.

2. EXPERIMENTAL

2.1. Chemicals

Graphite was purchased from Sigma Aldrich, Germany; potassium permanganate and ammoniac were purchased from ViNa Chemsol, Vietnam; sulfuric acid, acetone, ferric chloride ($\text{FeCl}_3 \cdot 6\text{H}_2\text{O}$), ferrous chloride ($\text{FeCl}_2 \cdot 4\text{H}_2\text{O}$), and nickel chloride ($\text{NiCl}_2 \cdot 6\text{H}_2\text{O}$) were purchased from Xilong Chemical, China. Well-deionized water was used in all experiments. All chemicals were used without further purification.

2.2. Synthesis of $\text{Fe}_3\text{O}_4/\text{GO}$ nanocomposites

GO was synthesized by modified Hummers' method [5]. Fe_3O_4 nanoparticles were prepared according to the modified

Massart's method [6] via the co-precipitation of a mixture of $\text{FeCl}_3 \cdot 6\text{H}_2\text{O}$ and $\text{FeCl}_2 \cdot 4\text{H}_2\text{O}$. After that, GO dispersion (0.3 g GO in 300 ml distilled water) was sonicated for 30 min. An amount of Fe_3O_4 nanoparticles (0.3 g) was added to the dispersion. After 30 min of sonication, to obtain an homogeneous suspension, the resulted nanocomposites were collected by magnet and then freeze-dried [7].

2.3. Characterization

X-ray diffraction (XRD) patterns were observed on a Bruker D8 Advanced powder diffractometer system using $\text{Cu-K}\alpha$ radiation ($\lambda = 1.54 \text{ \AA}$). Fourier transform infrared (FTIR) spectra were recorded in the $400\text{-}4000 \text{ cm}^{-1}$ range at a resolution of 4 cm^{-1} with a Bruker FTIR Alpha-E spectrometer. The morphology of the nanocomposite was investigated using a transmission electron microscope (TEM) JEOL JEM 1010 operating at 100 kV and equipped with a Gatan Orius SC600 CCD camera for digital imaging. TEM sample was prepared by dropping ethanol dispersion of $\text{Fe}_3\text{O}_4/\text{GO}$ on carbon-coated copper grids (200 mesh). The surface area of the nanocomposite was characterized by isothermal adsorption method (BET). The superparamagnetism of $\text{Fe}_3\text{O}_4/\text{GO}$ was presented by vibrating sample magnetometry (VSM). The adsorption capacity for Ni^{2+} ions was investigated by Langmuir model. The concentration of residual Ni^{2+} ions was measured by ultraviolet and visible spectra (UV-Vis).

2.4. Removal of Ni^{2+} ions

2.4.1 Effect of contact time

$\text{NiCl}_2 \cdot 6\text{H}_2\text{O}$ was used as the source of Ni^{2+} . A typical adsorption experiment was carried out by adding 0.05 g $\text{Fe}_3\text{O}_4/\text{GO}$ to a 50 ml Ni^{2+}

solution ($C_0 = 250$ mg/l) at room temperature (25°C). The pH of solution was adjusted about 6.5. After each particular time (5, 10, 20, 30, 40, 60, 120, 240, 360, 480, 540, 1440 mins), Ni (II) solution was collected with 0.5 ml. This specimen was measured by UV-Vis to determine Ni (II) concentration [8].

2.4.2 Effect of pH

A typical adsorption experiment was carried out by adding 0.02 g $\text{Fe}_3\text{O}_4/\text{GO}$ to a 20 ml Ni^{2+} solution ($C_0 = 250$ mg/l) at room temperature (25°C). The pH of solution was adjusted in the range of 2 to 8. After proper time, Ni (II) solution was collected with 0.5 ml. This specimen was measured by UV-Vis to determine Ni (II) concentration.

2.4.3 Langmuir isotherm for the adsorption of Ni^{2+}

A typical adsorption experiment was carried out by adding 0.02 g $\text{Fe}_3\text{O}_4/\text{GO}$ to a 20 ml Ni^{2+} solution at room temperature (25°C) under suitable pH and contact time. After that, $\text{Fe}_3\text{O}_4/\text{GO}$ was removed by using a magnet. Then, the residual solution was collected and analyzed. The initial concentration of Ni^{2+} solution was changed from 5 mg/l to 250 mg/l.

The Langmuir isotherm relationship is of a hyperbolic form:

$$q = q_m \frac{bC_f}{1+bC_f} \quad (1)$$

where q is sorption uptake; q_m is the maximum sorbate uptake under the given conditions; C_f is final equilibrium concentration of the residual sorbate remaining in the solution; b is a coefficient related to the affinity between the sorbate and sorbate.

3. EXPERIMENTAL

3.1. XRD patterns and FTIR spectrum

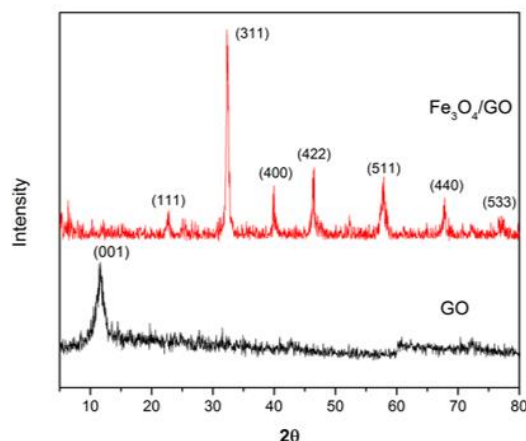


Figure 1. XRD patterns of $\text{Fe}_3\text{O}_4/\text{GO}$ and GO

As shown in Figure 1, for the XRD pattern of GO, the diffraction peak at $2\theta = 10.2^\circ$ can be confidently indexed as the (001) reflection of the GO [9]. For the XRD pattern of $\text{Fe}_3\text{O}_4/\text{GO}$, the intense diffraction peaks at $2\theta = 22.5^\circ$, 32.5° , 41.5° , 47.5° , 58° , 67° , and 77.5° represented the corresponding indices (111), (311), (400), (422), (511), (440), and (533) respectively [10]. Furthermore, the absence of the (001) reflection of the GO in XRD pattern of $\text{Fe}_3\text{O}_4/\text{GO}$ showed that GO layers were exfoliated completely.

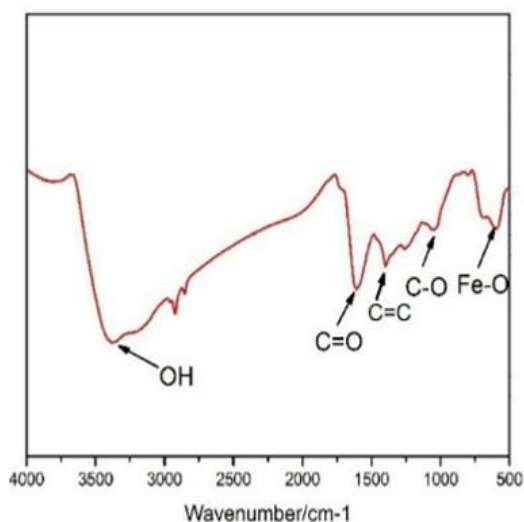


Figure 2. FTIR spectrum of $\text{Fe}_3\text{O}_4/\text{GO}$

Additionally, according to Figure 2, the spectrum of $\text{Fe}_3\text{O}_4/\text{GO}$ presented the broad band around 3380 cm^{-1} is assigned to O-H stretching vibration due to the method of sample preparation. The band at 1399 cm^{-1} was attributed to C=C stretching mode of the sp^2 carbon skeletal network. Carbonyl groups of GO were observed as bands at 1700 cm^{-1} , while the band at 1053 cm^{-1} was attributed to the stretching vibrations of C-O of epoxy groups. The spectrum of $\text{Fe}_3\text{O}_4/\text{GO}$ nanocomposite additionally presented the characteristic stretching vibration peak 596 cm^{-1} which proved that Fe_3O_4 nanoparticles were successfully anchored onto GO sheets. These results were proper with the prehistoric research [11].

3.2. TEM image and BET surface area

TEM observation was also undertaken to characterize the morphologies of the $\text{Fe}_3\text{O}_4/\text{GO}$ nanocomposite. As shown in Figure 3, Fe_3O_4 particles are agglomerated, evidenced by formation of large clusters. It can be distinctly seen that the Fe_3O_4 clusters were deposited onto GO surfaces of the nanocomposites. Moreover,

no isolated Fe_3O_4 clusters were observed beyond the GO, suggesting a strong interaction between the Fe_3O_4 clusters and GO sheets.

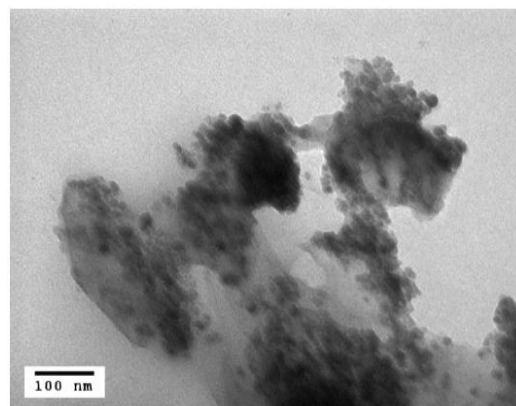


Figure 3. TEM images of $\text{Fe}_3\text{O}_4/\text{GO}$ nanocomposites

Additionally, TEM image also revealed that the size of the Fe_3O_4 nanoparticles was approximately 20-25 nm.

The BET specific surface area of $\text{Fe}_3\text{O}_4/\text{GO}$ was about $72.9\text{ m}^2/\text{g}$.

3.3. Magnetization

It can be seen at Figure 4 that $\text{Fe}_3\text{O}_4/\text{GO}$ nanocomposite could be easily separated under an external magnetic field. Without the magnet, the nanocomposite was dispersed in water. Using VSM method, the magnetic behaviors of $\text{Fe}_3\text{O}_4/\text{GO}$ were further investigated at room temperature in the field range of $-15 < H < +15$ kOe. Figure 5 shows magnetic hysteresis loops for $\text{Fe}_3\text{O}_4/\text{GO}$. The saturated magnetization for $\text{Fe}_3\text{O}_4/\text{GO}$ was 27.1 emu/g . This result is good compared with $\text{Fe}_3\text{O}_4/\text{GO}$ nanocomposites reported in references [12,13].

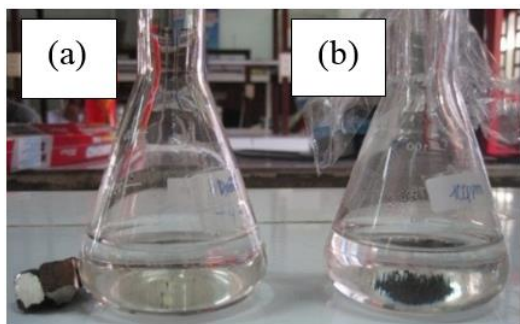


Figure 4. Digital photos of $\text{Fe}_3\text{O}_4/\text{GO}$ suspension (a) with and (b) without exterior magnetic field

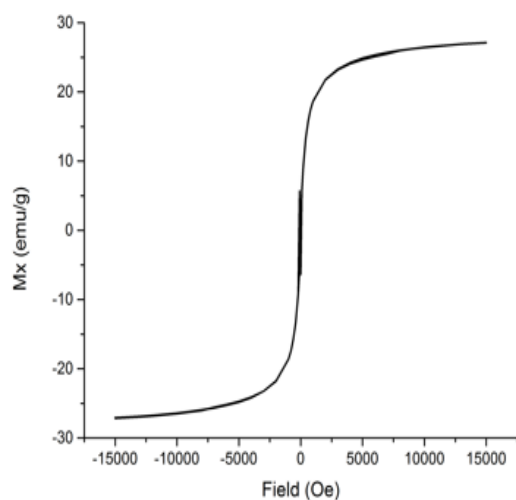


Figure 5. Magnetic hysteresis curve of $\text{Fe}_3\text{O}_4/\text{GO}$

3.4. Adsorption study

3.4.1 Effect of contact time

The effect of contact time on $\text{Fe}_3\text{O}_4/\text{GO}$ adsorption from solution is given in Figure 6. It can be seen that Ni (II) adsorption increases with increase of contact time, and a rapid adsorption is observed in 200 min. Based on these results, a contact time of 500 min was assumed to be suitable for the sorption experiments.

In order to determine Ni (II) adsorption kinetics, the pseudo-second-order kinetic model was investigated as follows:

$$\frac{t}{q_t} = \frac{1}{k_2 q_e^2} + \left(\frac{1}{q_e}\right)t \quad (2)$$

where q_t and q_e are total adsorbed amounts at time t and at equilibrium, respectively; k_2 he pseudo-second order constant.

According to this equation, the factors of adsorption kinetic of $\text{Fe}_3\text{O}_4/\text{GO}$ for nickel were revealed:

Table 1. The factors of adsorption kinetic

Temp. (°C)	pH	Pseudo-second-order equation		
		q_e (mg/g)	k_2 (min ⁻¹)	R^2
298	6.5	142.86	0.683	0.9649

As seen from Table I, the correlation coefficients (R^2) given by the pseudo-second-order kinetic is 0.9649. High regression correlation coefficient is suggesting that the adsorption nickel by $\text{Fe}_3\text{O}_4/\text{GO}$ was fitted with pseudo-second-order kinetic model.

Based on above discussion, the pseudo-second-order adsorption mechanism is predominant, meaning that chemical sorption takes part in the adsorption process.

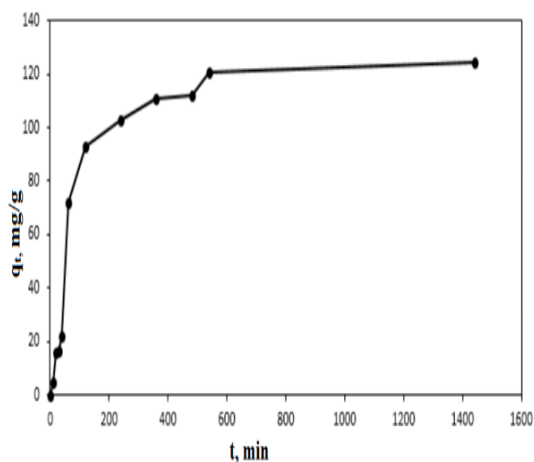


Figure 6. Effect of contact time on adsorption of Ni^{2+} by $\text{Fe}_3\text{O}_4/\text{GO}$

3.4.2 Effect of pH

Because hydrogen atom will compete with the positively charged metal ions on the active sites of the adsorbent in the solution, pH is considered as the most important parameter affecting metal ion adsorption [14]. The pH effects related to the sort and behavior of the adsorbent in the solution, together with the adsorbed ions sorts. It is observed that the adsorption of Ni (II) is strongly dependent on pH value. At pH 3-7, the sorption ability for all samples is low, meaning the competition of an excess of hydrogen ions with Ni (II) for bonding sites. At pH 2 and 8, the sorption increases sharply. The effect of pH can be explained by considering the surface charge of the $\text{Fe}_3\text{O}_4/\text{GO}$ and the degree of ionization and the species of nickel. It is well known that Ni (II) can present in the forms of Ni^{2+} , $\text{Ni}(\text{OH})^+$, $\text{Ni}(\text{OH})_2^0$, $\text{Ni}(\text{OH})_3^-$ in the solution. At pH < 7, the predominant nickel species is Ni^{2+} .

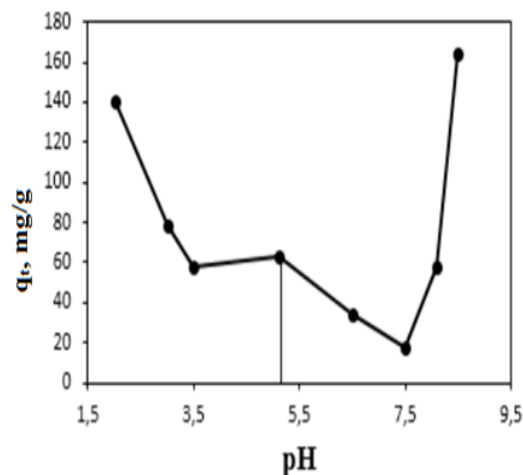


Figure 7. Effect of pH on adsorption of Ni^{2+} by $\text{Fe}_3\text{O}_4/\text{GO}$

Adsorption functional groups such as carboxyl or hydroxyl are negatively charged. Consequently, the electrostatic attraction of positively charged Ni (II) onto the adsorbents enhances the capacity greatly. At pH > 8.2, the maximum Ni (II) removal is attributed to the formation of hydrolysis species i.e. $\text{Ni}(\text{OH})^+$, $\text{Ni}(\text{OH})_2^0$ [15].

3.4.3 Langmuir isotherm model for the adsorption of Ni^{2+}

Adsorption isotherm is of fundamental importance in the design of adsorption system, which indicates how Ni (II) ions is partitioned between the adsorbent and liquid phases at equilibrium as a function of increasing ions concentration. Table II shows the Langmuir model for the nickel adsorption of $\text{Fe}_3\text{O}_4/\text{GO}$, Fe_3O_4 , and GO.

Table 2. Langmuir model

Materials	Langmuir		
	q_m (mg/g)	b (l/mg)	R^2
Fe ₃ O ₄ /GO	27.62	0.0977	0.9711
Fe ₃ O ₄	15.34	0.0543	0.9972
GO	68.97	0.0177	0.9623

And Figure 8 shows the comparison about the maximum adsorption capacity for nickel of three materials. As a result, Fe₃O₄/GO has the adsorption higher than Fe₃O₄. The nickel adsorption of GO is higher than Fe₃O₄ and Fe₃O₄/GO. However, Fe₃O₄/GO is more suitable for nickel removal because of its magnetism.

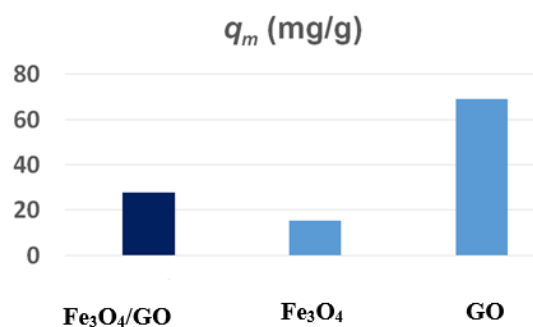


Figure 8. The comparison of q_m between Fe₃O₄/GO, GO, and Fe₃O₄

4. CONCLUSIONS

Fe₃O₄/GO nanocomposite was prepared and used as adsorbent for the removal of Ni (II) ions from aqueous solution. The maximum adsorption capacity of Fe₃O₄/GO is 27.62 mg/g with Fe₃O₄ particle size range of 20-25 nm. The adsorption data were fit well by the pseudo-second-order kinetic model and Langmuir model. The results presented in this work indicate that Fe₃O₄/GO nanocomposite as a promising adsorbent has great potential for the removal of metal ions from wastewater.

Acknowledgements: This work was supported by Vietnam National University, Ho Chi Minh City through the **TX2016-20-04/HĐ-KHCN** project.

Chế tạo, khảo sát đặc tính và khả năng hấp phụ niken của vật liệu nanocomposite Fe_3O_4 /graphene oxide

- Nguyễn Hữu Hiếu
- Hoàng Minh Nam
- Phan Thị Hoài Diễm

Trường Đại học Bách Khoa, ĐHQG-HCM

TÓM TẮT

Trong nghiên cứu này, graphene oxide (GO) được tổng hợp bằng phương pháp Hummers cải biên và vật liệu nanocomposite Fe_3O_4 /GO được tổng hợp theo phương pháp phối trộn huyền phù. Hình thái-cấu trúc-đặc tính của vật liệu được khảo sát bởi nhiễu xạ tia X, phổ hồng ngoại chuyển tiếp Fourier, kính hiển vi điện tử truyền qua, diện tích bề mặt riêng BET và từ kế mẫu rung. Nồng độ ion Ni

(II) trong dung dịch được xác định bằng máy đo quang phổ tử ngoại-khả kiến. Khả năng hấp phụ ion Ni (II) của vật liệu nanocomposite được đánh giá qua sự ảnh hưởng của pH, số liệu động học và cân bằng đẳng nhiệt theo các mẻ thí nghiệm. Dung lượng hấp phụ tối đa đối với ion Ni (II) ở nhiệt độ phòng của vật liệu Fe_3O_4 /GO được ước tính theo mô hình đẳng nhiệt Langmuir là 27,62 mg/g.

Từ Khóa: Fe_3O_4 , graphene oxide, nanocomposit, hấp phụ, niken.

REFERENCES

- [1]. Dreyer S.P.D.R, C.W. Bielawski, R.S. Ruoff. The chemistry of graphene oxide. Chem. Soc. Rev., vol.39, pp.228–240, (2010).
- [2]. V. Skákalová and A. B.Kaiser, GE properties, prepare, characterisation and devices, Woodhead Publishing, 2014.
- [3]. V. Dhand, et al.A Comprehensive Review of GE Nanocomposite: Research Status and Trends. Journal of Nanomaterials, vol.2013, pp.1-14, (2013).
- [4]. W. Zhang, et al. Synthesis of water-soluble magnetic graphene nanocomposites for recyclable removal of heavy metal ions. Journal of Materials Chemistry A, vol.1, pp.1745-1753, (2013).
- [5]. A.A. L. Shahriary, and Athawale. Graphene Oxide Synthesized by using Modified Hummers Approach. International Journal of Renewable Energy and Environmental Engineering, vol.2, pp.58-63, (2014).

- [6]. R. Masart. Preparation of aqueous magnetic liquids in alkaline and acidic media. *IEEE Transactions on Magnetism*, vol.17, pp.1247-1248, (1981).
- [7]. G.Z. Kyzas, E.A. Deliyanni, and K.A. Matis. Graphene oxide and its application as adsorbent to wastewater treatment. *Journal of Chemical Technology & Biotechnology*, vol.89, pp.196-205, (2013).
- [8]. Y. Ren, N. Yan, and Q. Wen. Graphene/ δ - MnO_2 composite as adsorbent for the removal of nickel ions from wastewater. *Chemical Engineering Journal*, vol.175, pp.1-7, (2011).
- [9]. C. Xu and X. Wang. Fabrication of Flexible Metal-Nanoparticle Films Using Graphene Oxide Sheets as Substrates. *Small*, vol.5, pp.2212-2217, (2009).
- [10]. Y. Todaka, M. Nakamura, and S. Hattori. Synthesis of Ferrite Nanoparticles by Mechanochemical Processing Using a Ball Mill. *Materials Transactions*, vol.44, pp.277-284, (2003).
- [11]. T.K. Das and S. Prusty. Graphene – based polymer composites and their applications. *Polymer- Plastics Tech & Eng*, vol.52, pp.319-331, (2013).
- [12]. Y.W. Liu, M.X. Guan, and L. Feng. Facile and straightforward synthesis of superparamagnetic reduced graphene oxide- Fe_3O_4 hybrid composite by a solvothermal reaction. *Nanotechnology*, vol.24, (2013).
- [13]. M. Liu, C. Chen, and J. Hu. Synthesis of Magnetite/Graphene Oxide Composite and Application for Cobalt(II) Removal. *J. Phys. Chem. B*, 115, pp.25234–25240, (2011).
- [14]. V. Srivastava, et al. Adsorption of Nickel Ions from Aqueous Solutions by Nano Alumina: Kinetic, Mass Transfer, and Equilibrium Studies. *J. Chem. Eng. Data*, vol.56, pp.1414-1422, (2011).
- [15]. Y. Xing, et al. Sonochemical oxidation of multiwalled carbon nanotubes. *Langmuir*, vol.21, pp.4185-4190, (2005).